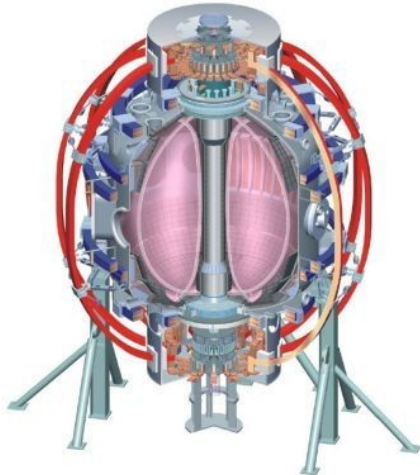


Overview of NSTX divertor and plasma-material interactions, diagnosis and modeling

M.A. Jaworski, T. Abrams, M.G. Bell, R. Kaita, J. Kallman, H. Kugel, B. LeBlanc, R. Maqueda, D. Stotler, S. Zweben (PPPL), E. Foley, F. Levinton (Nova Photonics), V. Surla (UIUC), J.D. Elder (U-Toronto), T.K. Gray, R. Maingi, A. McLean (ORNL), and V. Soukhanovskii (LLNL)

**52nd American Physical Society Division of Plasma Physics Meeting
 Chicago, IL, November 8th, 2010**



*College W&M
 Colorado Sch Mines
 Columbia U
 CompX
 General Atomics
 INEL
 Johns Hopkins U
 LANL
 LLNL
 Lodestar
 MIT
 Nova Photonics
 New York U
 Old Dominion U
 ORNL
 PPPL
 PSI
 Princeton U
 Purdue U
 SNL
 Think Tank, Inc.
 UC Davis
 UC Irvine
 UCLA
 UCSD
 U Colorado
 U Illinois
 U Maryland
 U Rochester
 U Washington
 U Wisconsin*

*Culham Sci Ctr
 U St. Andrews
 York U
 Chubu U
 Fukui U
 Hiroshima U
 Hyogo U
 Kyoto U
 Kyushu U
 Kyushu Tokai U
 NIFS
 Niigata U
 U Tokyo
 JAEA
 Hebrew U
 Ioffe Inst
 RRC Kurchatov Inst
 TRINITY
 KBSI
 KAIST
 POSTECH
 ASIPP
 ENEA, Frascati
 CEA, Cadarache
 IPP, Jülich
 IPP, Garching
 ASCR, Czech Rep
 U Quebec*

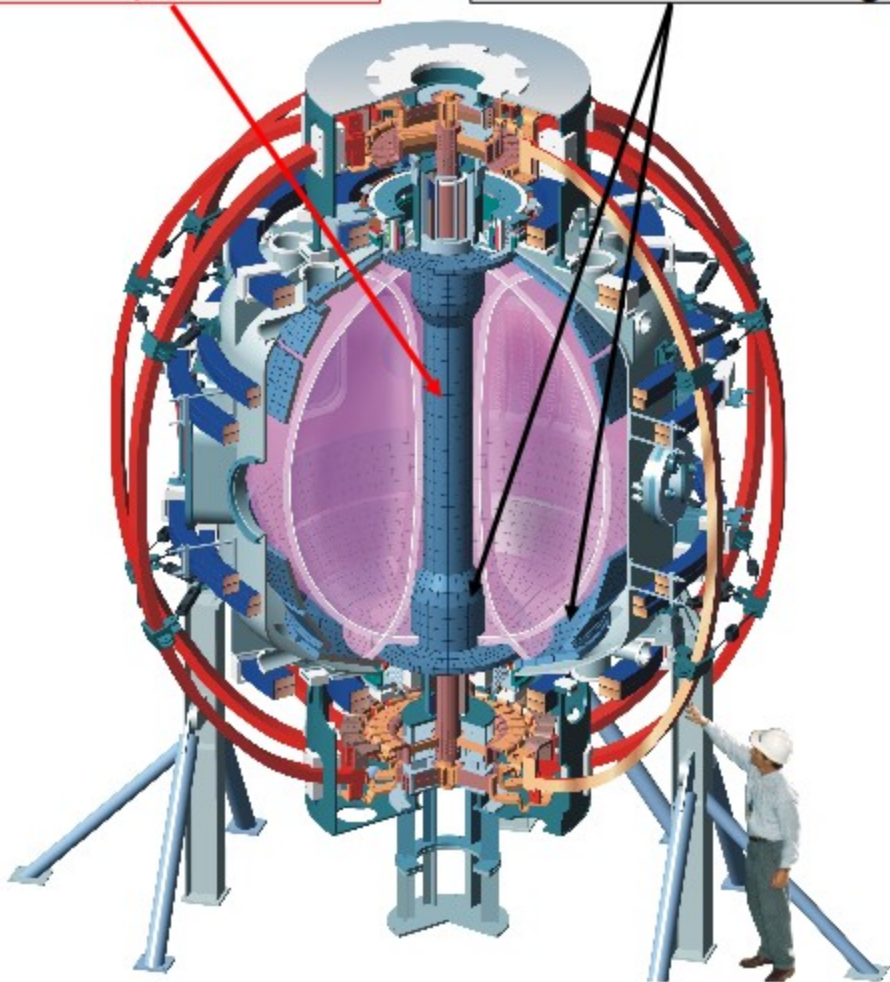
Overview

- Lithium operations in NSTX and boundary issues
- Diagnosis of SOL with Langmuir probe array
 - Hardware
 - Some initial results
 - Initial 2-point modeling of the SOL
- Dynamic plasma facing components (PFCs) in NSTX
- OEDGE interpretive modeling of NSTX
- Building a material model to inform NSTX-U decisions

NSTX Overview of Plasma Parameters

*Slim center column
with TF, OH coils*

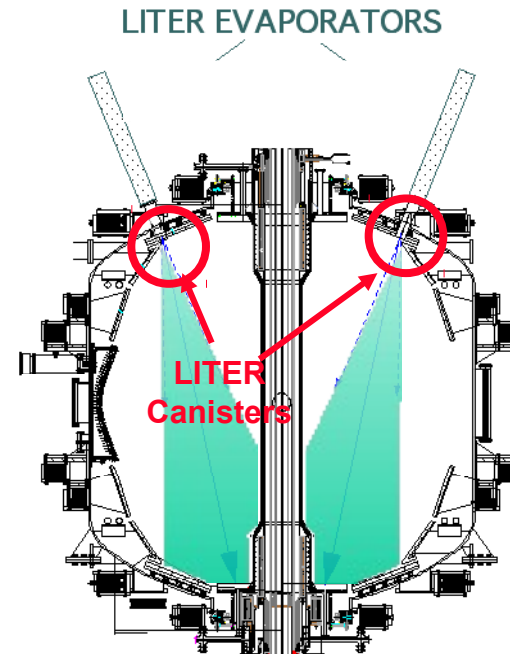
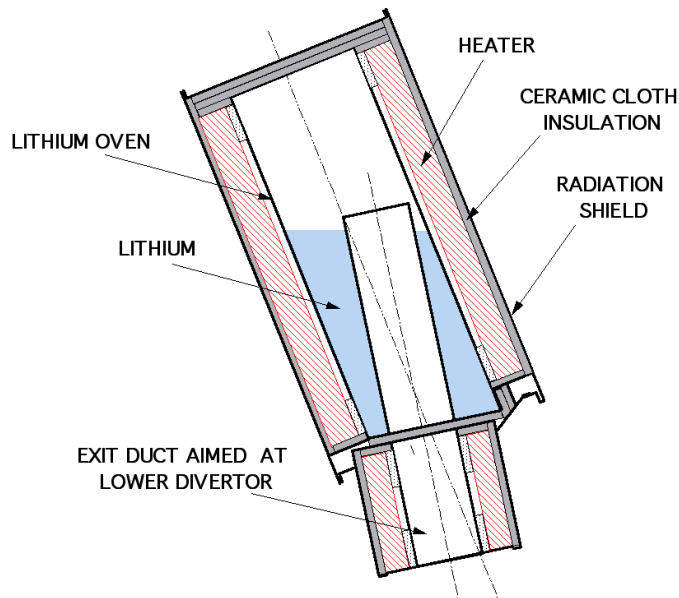
*Graphite/CFC PFCs
with lithium coating*



Aspect ratio A	1.27 – 1.7
Elongation κ	1.8 – 3.0
Triangularity δ	0.2 – 0.8
Major radius	0.85 m
Toroidal Field B_{T0}	0.4 – 0.55 T
Plasma Current I_p	0.7 – 1.5 MA
Auxiliary heating:	
NBI (100kV)	7 MW
RF (30MHz)	6 MW
Central temperature	1 – 5 keV
Central density	$\leq 1.2 \times 10^{20} \text{m}^{-3}$
Toroidal beta β_T	10 – 40 %

Lithium Deposition via Evaporation

- Electrically-heated stainless-steel canisters with re-entrant exit ducts
- Mounted 150° apart on probes behind gaps between upper divertor plates
- Each evaporates 1 – 40 mg/min with lithium reservoir at 520 – 630°C
- Deposits lithium on lower plasma facing surfaces
- In regular use since 2006



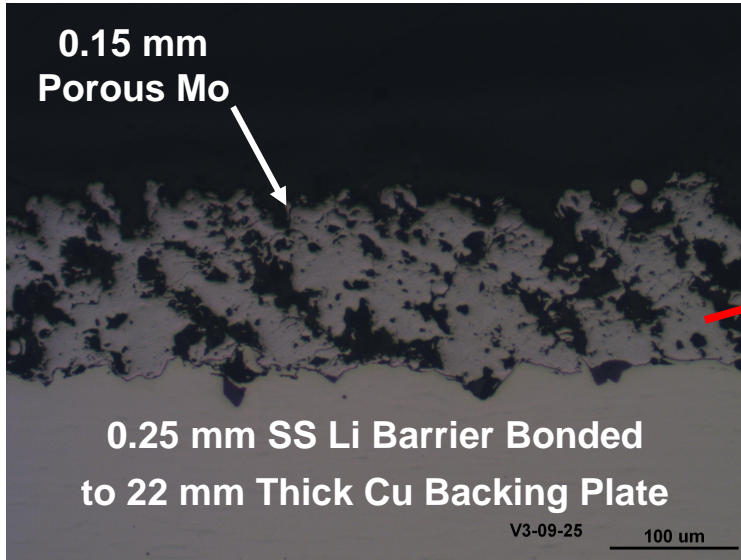
H. Kugel

Lithiated Graphite Wall Conditions Transient

- Control room experience indicates that after 2-3 discharges, benefits of lithium-coated PFCs wanes
 - LITER evaporation rate limited
 - Shot cycle time finite
 - Limited coatings possible during regular operations
- Clean, macroscopic liquid lithium predicted to have very low recycling coefficient
 - CDX-U demonstrated improved energy confinement with large-area liquid lithium limiter (Majeski, PRL, 2006)
 - See also LTX posters in session CP9 (this afternoon).
- Motivates the installation of the liquid lithium divertor in NSTX

Liquid Lithium Divertor

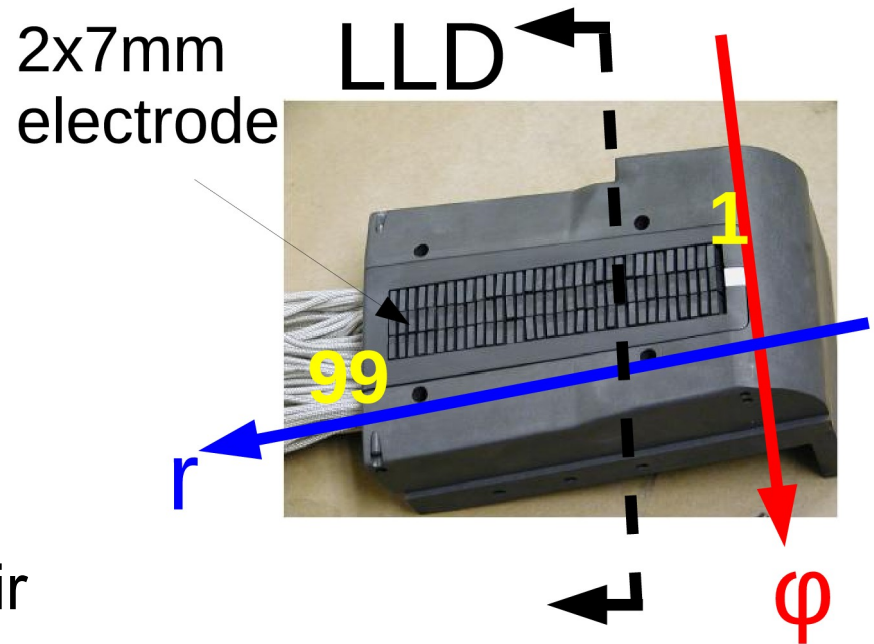
Micrograph of porous Mo layer



- Result of collaboration with Sandia National Laboratories
- Consists of flame-sprayed Mo surface on a thin stainless steel barrier covering a thick copper substrate
- Loaded via LITER evaporation from above
- Temperature controlled
- See H. Kugel - BP9.00041

New Langmuir Probe Array

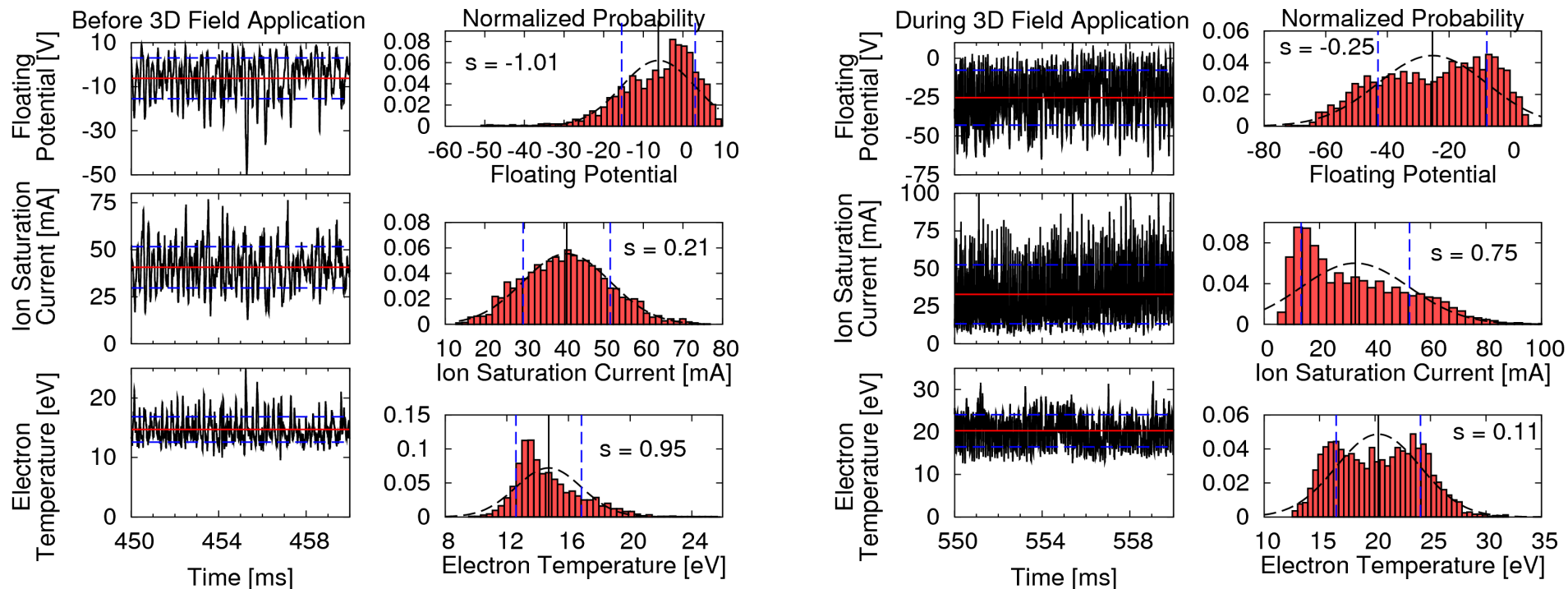
- Dense array of electrodes provides high spatial resolution
- Radially covers the LLD inboard leading edge
- Collaborative effort with U-Illinois
- Partially filled with standard swept probes, triple Langmuir probes and scrape-off-layer current monitors
- See also: J. Kallman BP9.00042 and V. Surla BP9.00046



J. Kallman, RSI, 2010
M.A. Jaworski, RSI, 2010

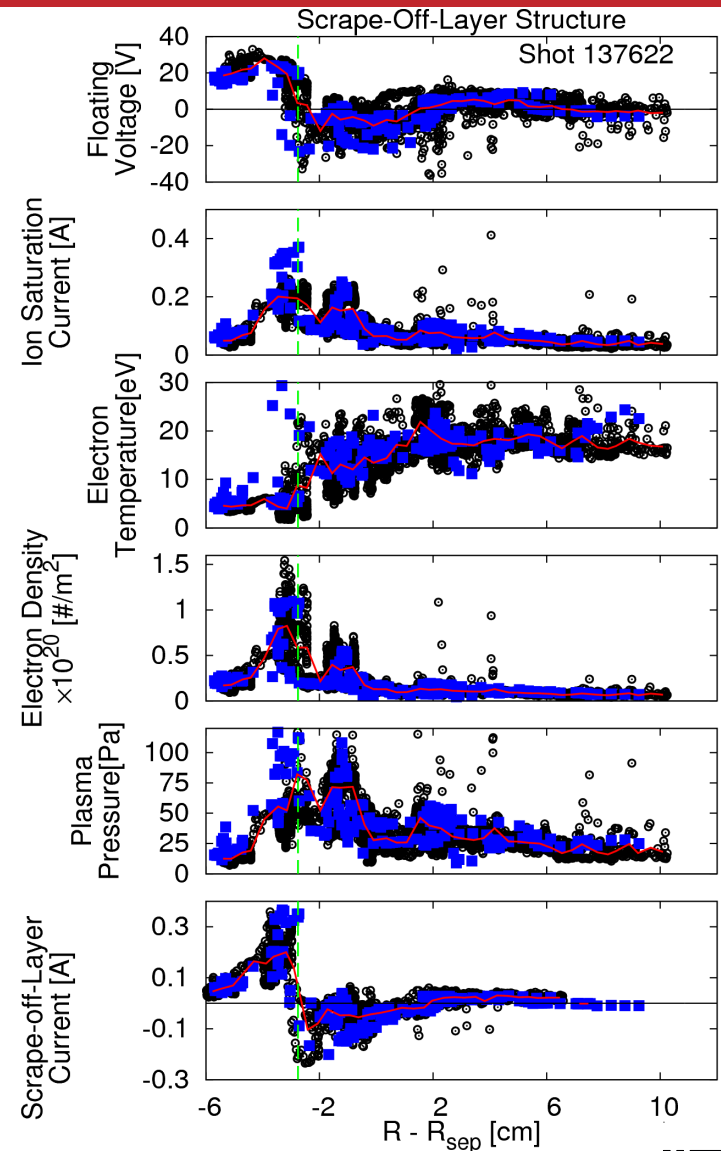
Triple Probes Complement Existing Turbulence Diagnostics

- Data example before and during application of 3D fields
- Probability density functions altered, as well as frequency
- Electron temperature becomes bi-modal
- Impact on single-probe interpretation being assessed



SOL Structure Obtained During Strike Point Sweeps

- Probe positions referenced to magnetic reconstruction
 - **Blue** points = single probe
 - **Black** points = triple probe or SOLC probe
 - **Red** line = Binned average
- Allows SOL structure to be obtained during a strike-point sweep over the array
- Provides additional means of locating the **separatrix**
 - V_F zero-crossing coincides with SOLC zero-crossing and
 - Peak pressure corresponds to this location

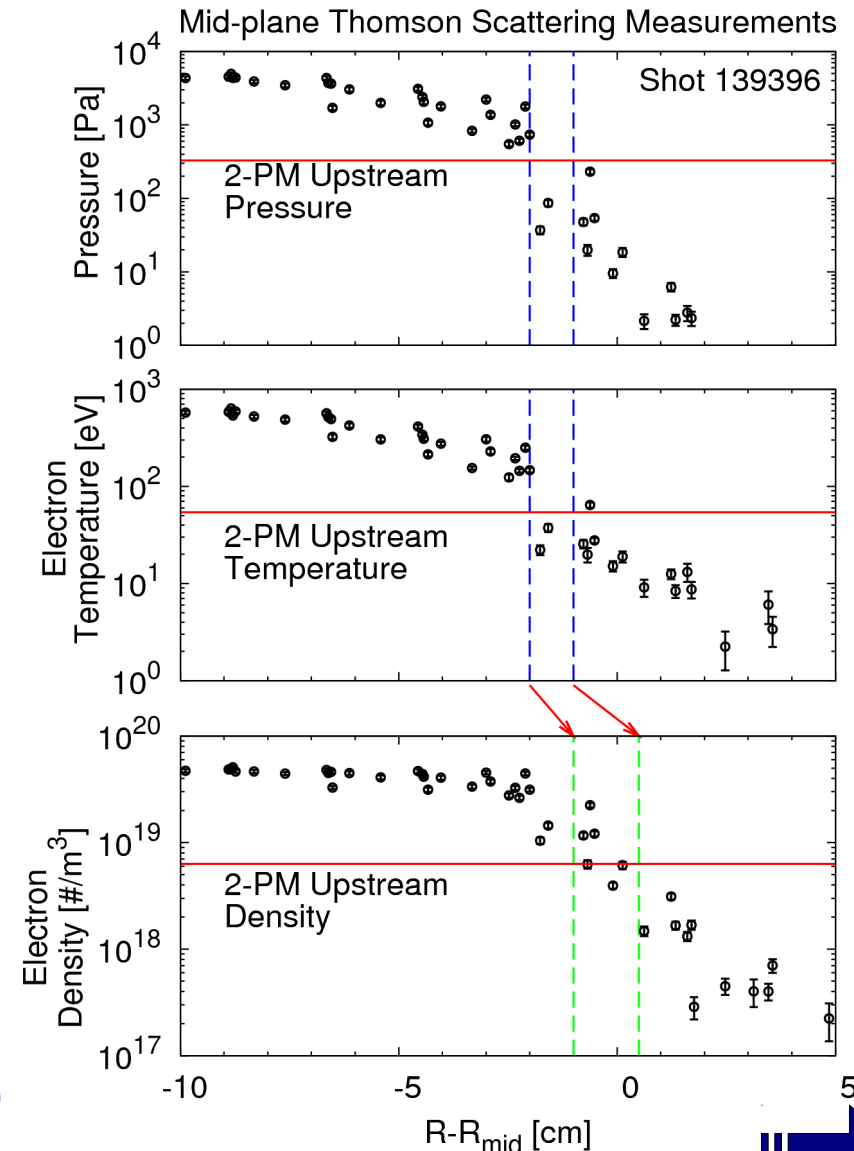


Importance of SOLC in PMI processes

- Local floating potential and SOLC intimately tied
 - Floating potential must adjust to be consistent with currents flowing through plasma
 - Equivalent to biasing the PFC to drive a current
- Enhanced sputtering in regions of positive current
 - Sheath potential energy enhanced by additional voltage between PFC and floating
 - Depending on Z of ion, impact energy can be greatly enhanced
- Enhanced heat flux in regions of negative current
 - Electrons carry bulk of plasma energy
 - Alters sheath heat transmission coefficient in the positive direction
 - Exponentially grows as surface voltage approaches plasma potential
 - Modest increase in sheath heat transmission occurs for positive current regions as well through enhanced ion energy

Upstream Separatrix Location Determined by Two-Point Model

- Simple 2-point model applied to SOL
 - Balances particle, momentum and energy in a flux tube
 - Define peak pressure along the target as the “real” separatrix location
 - Heat flux calculated with **probe data** (including floating potential effects)
 - Connection length obtained from TRACER code and magnetic soln.
 - Thomson scattering at midplane provides profile data
- Consistent location found with pressure and temperature
 - Density via 2-PM is low
 - Location improved with OSM integration (below) – discrepancy most likely due to magnetic variation in flux tube



What is the 2-Point Model?

- Models SOL flux tube
 - Straightened out plasma
 - No B variation
 - No radiative losses (in simple 2-PM)
 - Power enters at one end
- Balance pressure and power through flux tube
 - Assumes classical parallel-conductivity
 - Assume perfect recycling at the wall and particle balance on the flux tube
- Target power deposition modified with biased target sheath heat transmission

$$2n_t T_t = n_u T_u \quad \text{Flux tube pressure balance}$$

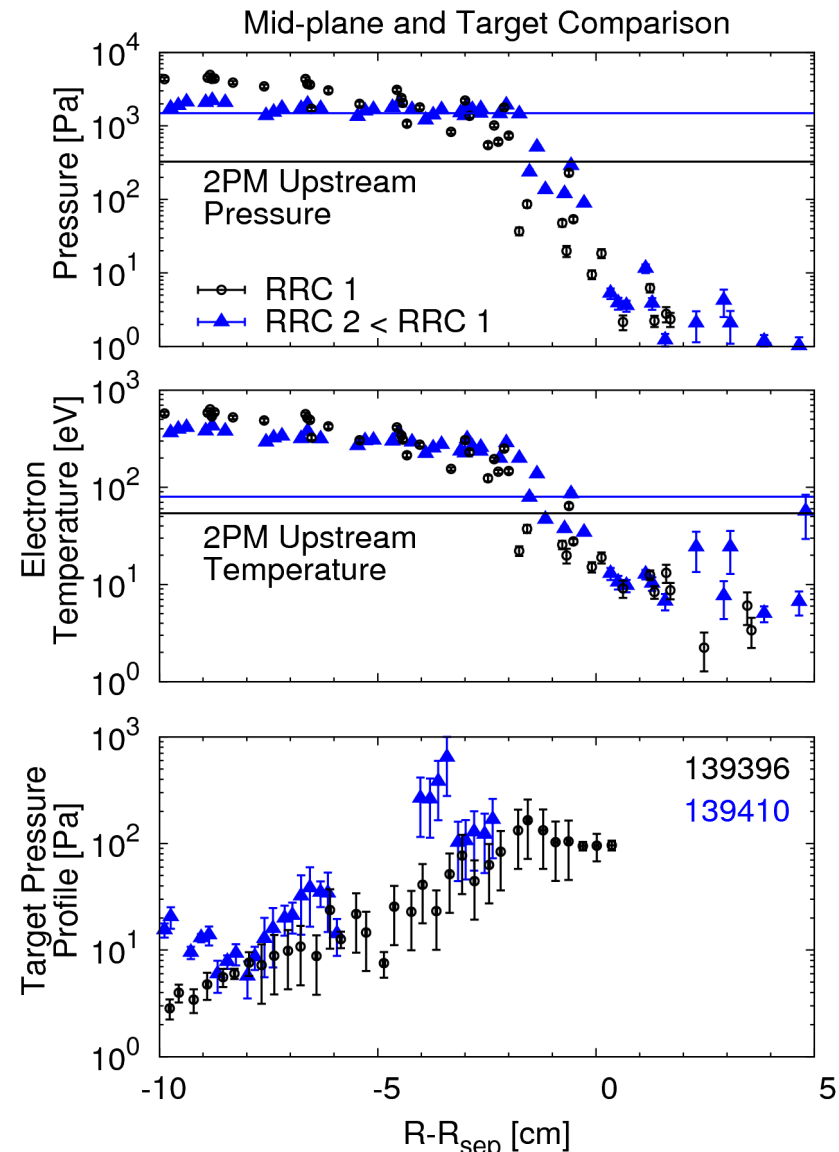
$$T_u = \left[T_t^{7/2} + \frac{7}{2} \frac{q_{\parallel} L}{2\kappa_{0e}} \right]^{2/7} \quad \text{Flux tube power balance}$$

$$q_{\parallel} = \gamma(V_s) n_t k T_t c_{st} \quad \text{Target power deposition}$$

$$\gamma(V_s) = -\frac{eV_s}{kT_e} + 2.5 \frac{T_i}{T_e} + 2 \left[\left(1 + \frac{T_i}{T_e} \right) \left(\frac{2\pi m_e}{m_i} \right) \right]^{-1/2} \exp\left(\frac{eV_s}{kT_e} \right)$$

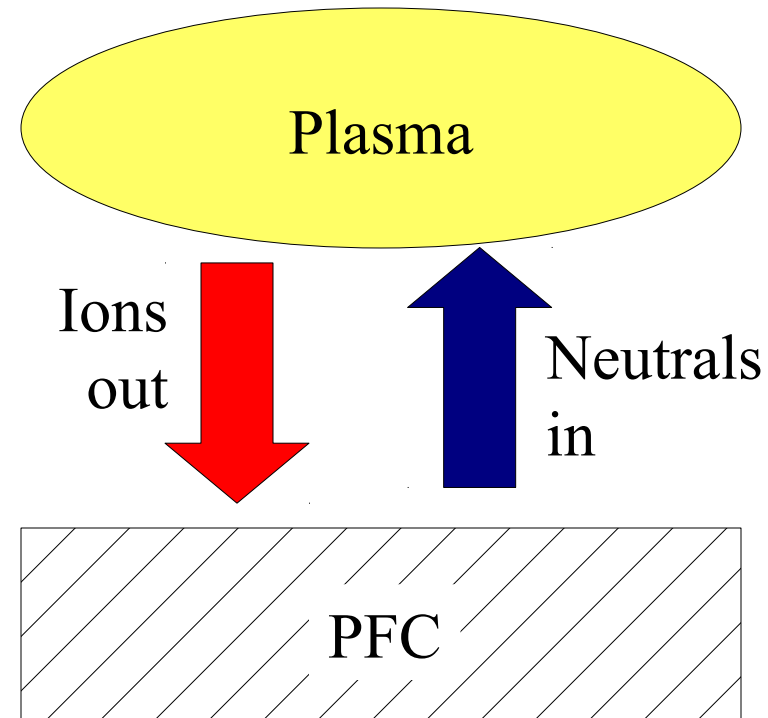
Two-Point Model Comparison of two LLD discharges

- Divertor profile exhibits higher pressure
 - $P_{t,peak} = 170$ Pa in 139396
 - $P_{t,peak} = 740$ Pa in 139410
 - Temperatures are comparable, but density is much larger in 139410
 - Mixture of effects – increased gas fueling, reappearance of type V ELMs
- Resulting upstream temperature is higher
 - $T_u = 54$ eV in 139396
 - $T_u = 80$ eV in 139410
- However, 2-PM is too simple
 - T_u is robust over a large set of parameters, but pressure and density affected by radiation and neutral momentum loss
 - Full strike-point profile not obtained in this discharge



Local Recycling Measurement

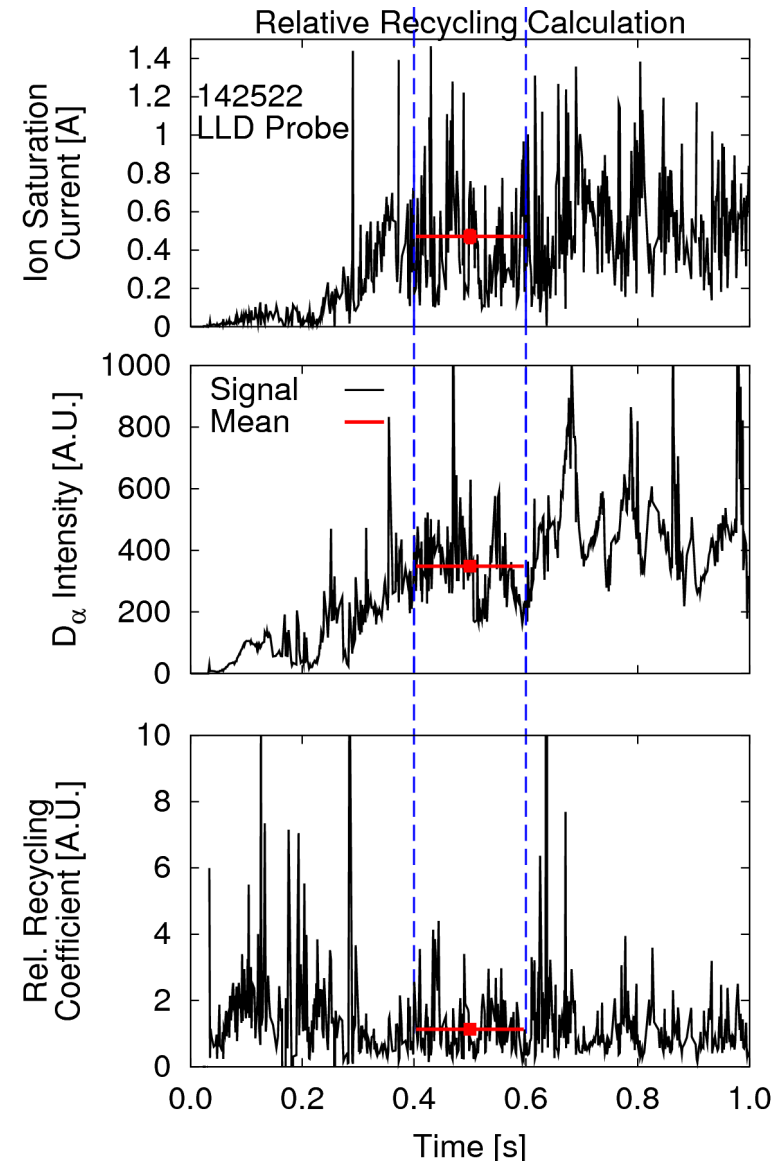
- Utilizes Langmuir probes and 1D-CCD camera D-alpha emission
 - D-alpha emission at PFC due to recycling neutrals
 - I_{sat} directly measures ion flux to probes
- Ratio provides recycling coefficient, however...
- Plasma geometry, radiation profile and reflections create significant uncertainty
 - Therefore, use the ratio in D-alpha intensity to I_{sat} as a *relative* recycling coefficient
- Relative recycling coeff. (RRC) allows trend analysis, but not absolute recycling coeff. determination



$$R = \frac{\text{Flux into plasma}}{\text{Flux into PFC}} \propto \frac{D_{\alpha} \text{ Intensity}}{I_{sat}^+}$$

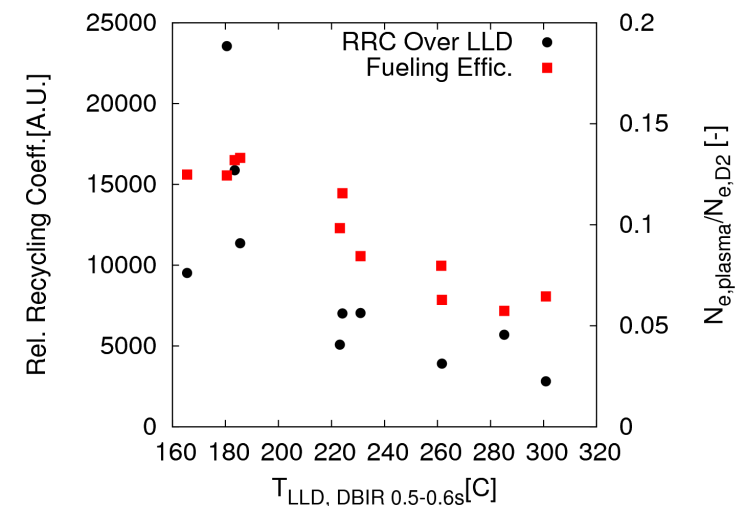
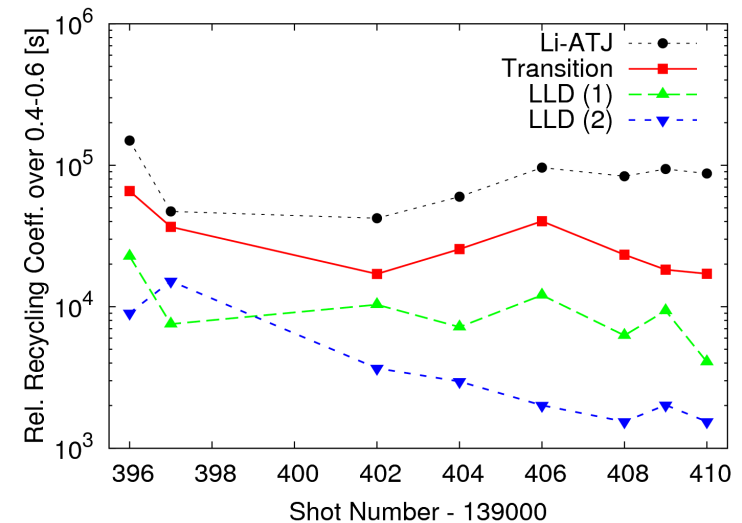
Example Relative Recycling Coefficient Calculation

- Plasma diverts after 200ms
- Achieves stable shape by 400ms
- Measurement made during stationary discharge period from 400-600ms (mean of signal)
- Same discharge shape in both shots
 - During first experiment, fueling rate increased (would tend to increase RRC)
 - In PFZ, dependent on PFCs on both sides of the flux tube (i.e. inboard and outboard – but both still Li-ATJ)
 - Motivates more rigorous work with OEDGE to take into account X-point and divertor leg radiation



Recycling Evolution During LLD Heating by Plasma

- During shot sequence, plasma heated the LLD
 - Melting point of Li = 180C
 - Gas puff rate increased during scan
 - Z_{eff} of carbon decreased
- Spatial variation of probes provides measurement at different PFCs
 - Probe 1 over Li-ATJ
 - Probe 2 at transition
 - Probes 3 and 4 over LLD
- Downward trend as run progressed visible in LLD probes,
 - Less apparent on Li-ATJ
 - Correlated with fueling efficiency decrease, and
 - Trends downward with temperature
 - But fueling was increased in sequence
 - Changes in both I_{sat} and D_{α}



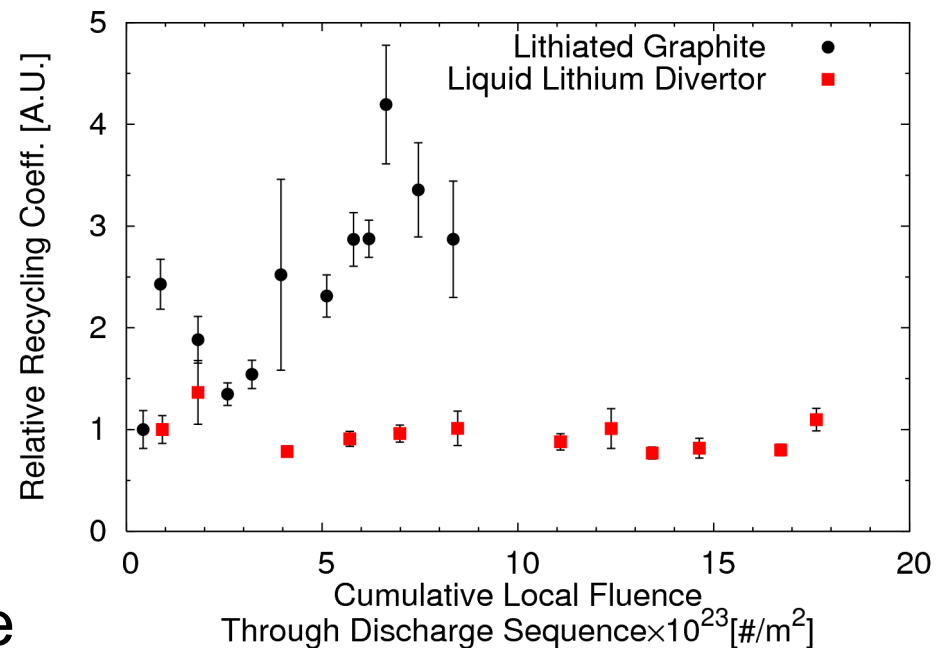
A. McLean – DB-IR
M. Bell – Fueling Eff.

Lithiated Graphite Exhibited Increase in Recycling

- Single LITER evaporation of 7.5gm
 - Plasma shape and fueling comparable
 - Discharges repeated through entire day
- Systematic rise in relative recycling coefficient on lithiated graphite, but not on the LLD
- Multi-shot ion fluence indicates LLD has “reservoir” effect compared to Li-graphite

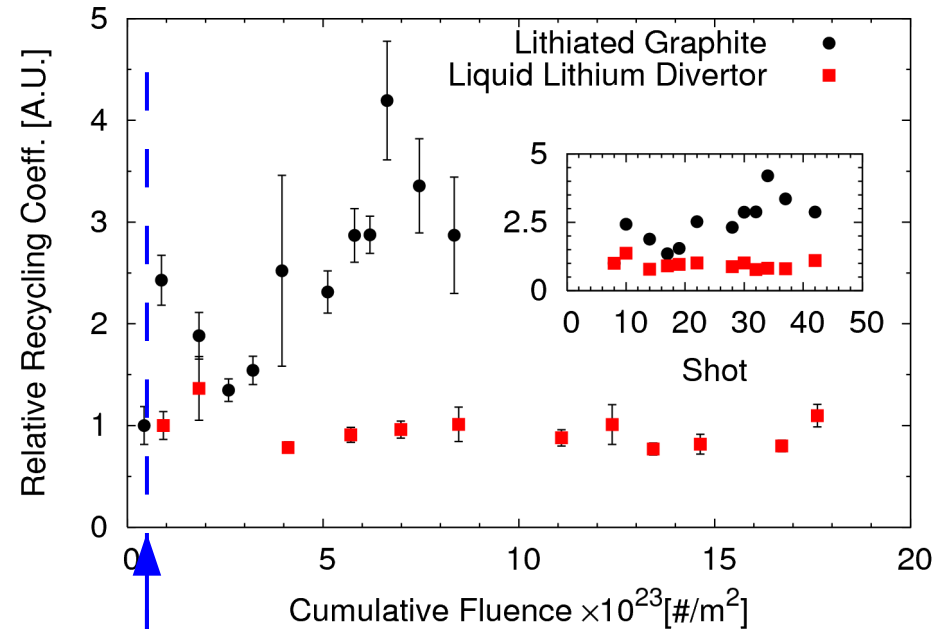
$$R = \frac{\text{Flux into plasma}}{\text{Flux into PFC}} \propto \frac{D_\alpha \text{ Intensity}}{I_{sat}^+}$$

$$N_{inc} = \text{Cumulative Fluence} \\ = \sum_{Shots} \left(\int \frac{I_{sat}^+}{eA_{probe}} dt \right)$$



Simplified Model for Recycling and Material Saturation

- PISCES-B data showed that Li absorbs D until converted to LiD (M. Baldwin, NF, 2002)
- LITER evaporation deposited 7.5gm, but amounts to $3.5 \times 10^{22} \text{ \#/m}^2$ in vicinity of LLD
- Simple fluence comparison would suggest the PFC should be saturated within the first discharge...
- Yet recycling continues to trend upward



Equivalent number density of deposited Li

$$N_{dep} \approx \frac{\eta m_{Li}}{\pi (R_o^2 - R_i^2)} \cdot \frac{A_v}{M_{Li}}$$

$$N_{dep} \approx \frac{0.05 \cdot 7.5 \text{ gm}}{0.9425 \text{ m}^2} \cdot \frac{6.022 \times 10^{23} \text{ \#/mol}}{6.941 \text{ gm/mol}}$$

$$N_{dep} \approx 3.5 \times 10^{22} \text{ \#/m}^2$$

Simple Model of Recycling as Function of Saturation

- Define saturation level, θ
- Assume recycling proportional to saturation level
- Only 1-R particles are absorbed
- Solve ODE for saturation as a function of incident fluence

$$\theta = \frac{N_D}{N_{Li}} \quad 0 \leq \theta \leq 1$$

$$R(\theta) = \frac{R_{max} - R_{min}}{\theta_{max} - \theta_{min}} \theta + R_{min} = \frac{\Delta_R}{1} \theta + R_{min} \quad R_{max} \leq 1$$

$$\frac{dN_D}{dt} = [1 - R(\theta)] \Gamma_{inc}$$

$$\frac{d\theta}{dt} = [1 - R(\theta)] \frac{\Gamma_{inc}}{N_{Li}}$$

$$N_{inc} = \Gamma_{inc} \cdot t$$

$$\theta(N_{inc}) = \frac{(1 - R_{min})}{\Delta_R} \left[1 - \exp \left(- \frac{N_{inc} \Delta_R}{N_{Li}} \right) \right]$$

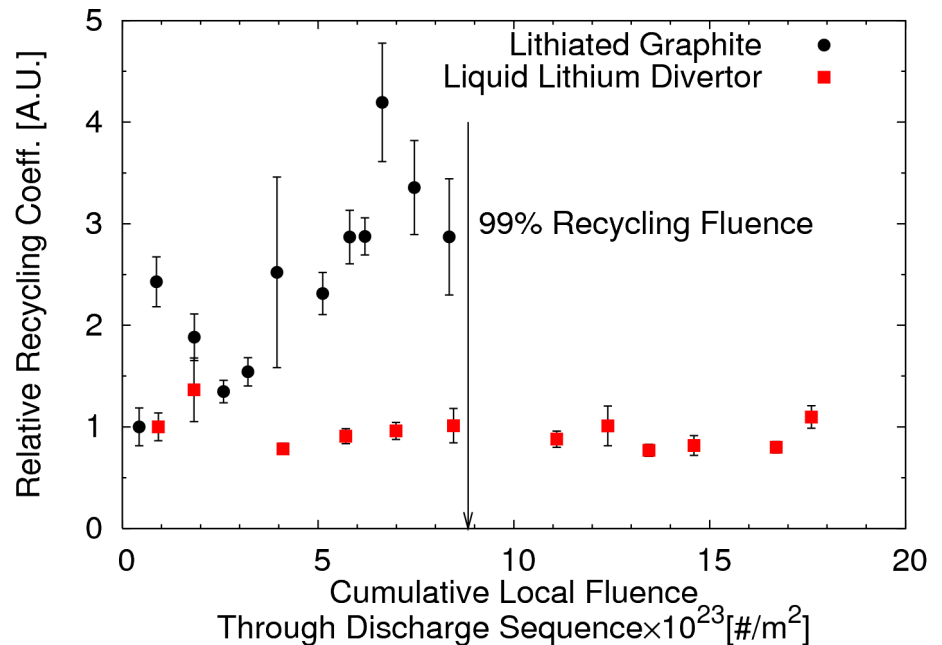
Can Predict 99% Recycling Fluence

- Change in saturation slows exponentially as material fills up
- Fluence to reach 99% recycling surface calculated as about 26 times the available lithium deposited
 - Assumes $R_{min} = 0.90$ from J. Canik SOLPS modeling
 - $R_{max} = 1.0$
 - Predicts the Li-ATJ may have more pumping ability beyond what was tested

$$0.99 = R(\theta_{99} = 0.9) \quad \text{for } R_{min} = 0.90$$

$$N_{inc}|_{R=0.99} = \frac{1}{\Delta_R} \ln \left(\frac{1}{1 - \theta_{99}} \right) \cdot N_{Li}$$

$$N_{inc}|_{R=0.99} \approx 25.6 \times N_{Li}$$

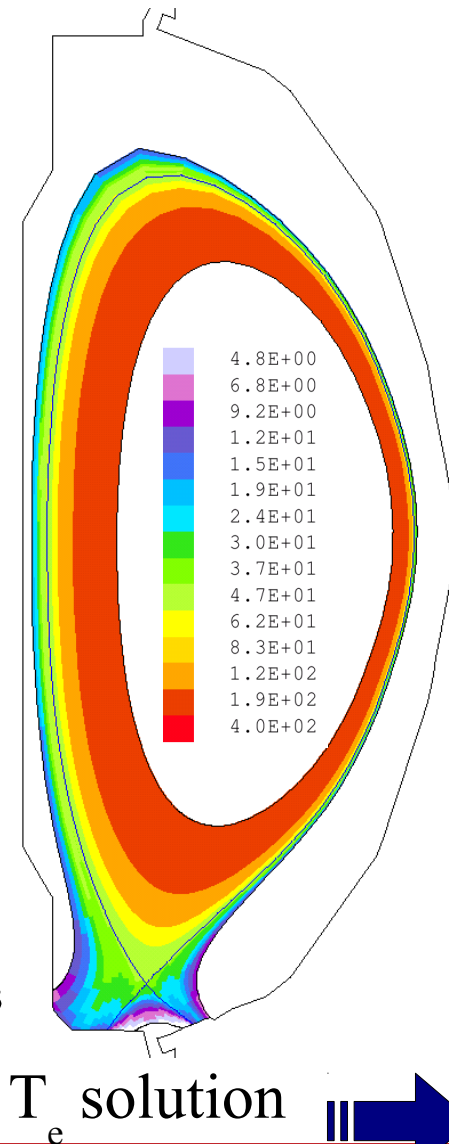
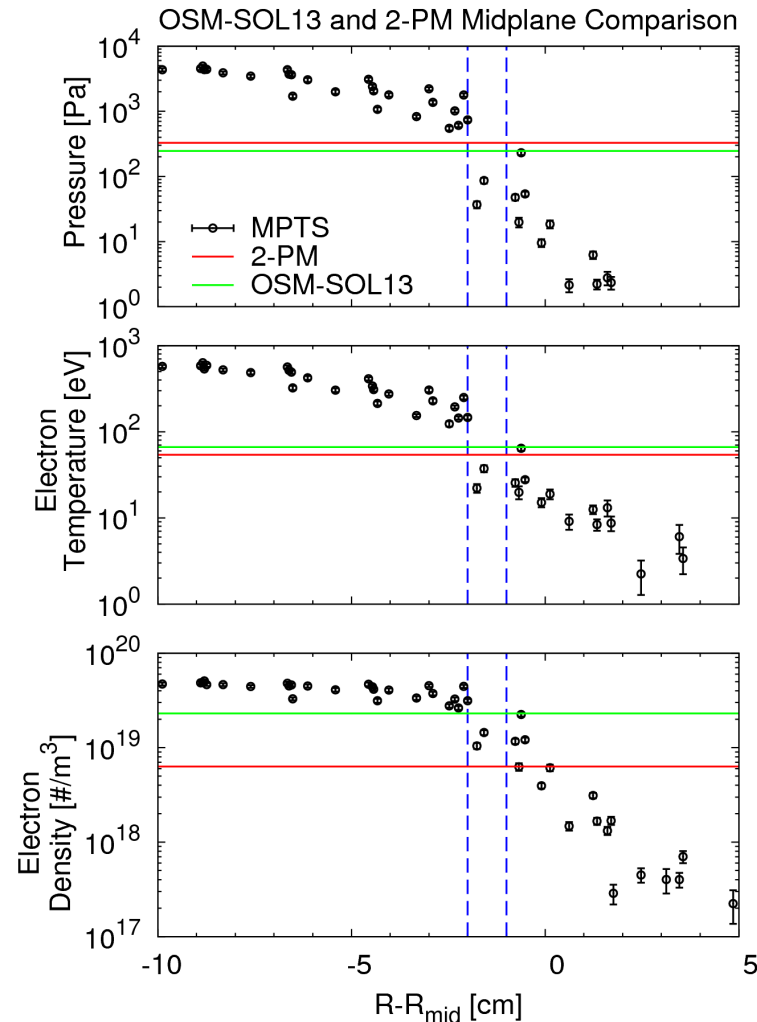


More Rigorous Analysis Available with OEDGE code suite

- Confront your model with *all* available data simultaneously
- Onion-skin method (OSM)
 - Generalization of the 2-point model – integrates fluid equation along a flux-tube
 - Assumes parallel transport \gg perpendicular
 - Allows individual flux-tube solution
- Eirene
 - Neutral transport code
 - Determines background neutral pressure in machine and interaction with plasma solution
 - Takes a wall model as input for calculating the recycling from the surface
- DIVIMP
 - Monte Carlo impurity model – utilizes sputtering tables to determine launch probabilities – tracks impurities and radiation cause by them

OSM Temperature Integration Improves Upstream Separatrix Location

- Separatrix location consistent in all three quantities
 - Mid-plane density finds consistent separatrix location with T_e and P_e
- Testcase run to develop work flow (proof-of-principle test)
 - Outboard Ne and Te obtained by probes
 - Core profile determined by MPTS
 - Inboard profile mimicked for this test case
 - Plasma solution found via pseudo-self consistent fluid model along flux-tubes
 - No neutral solution yet, simple ionization model

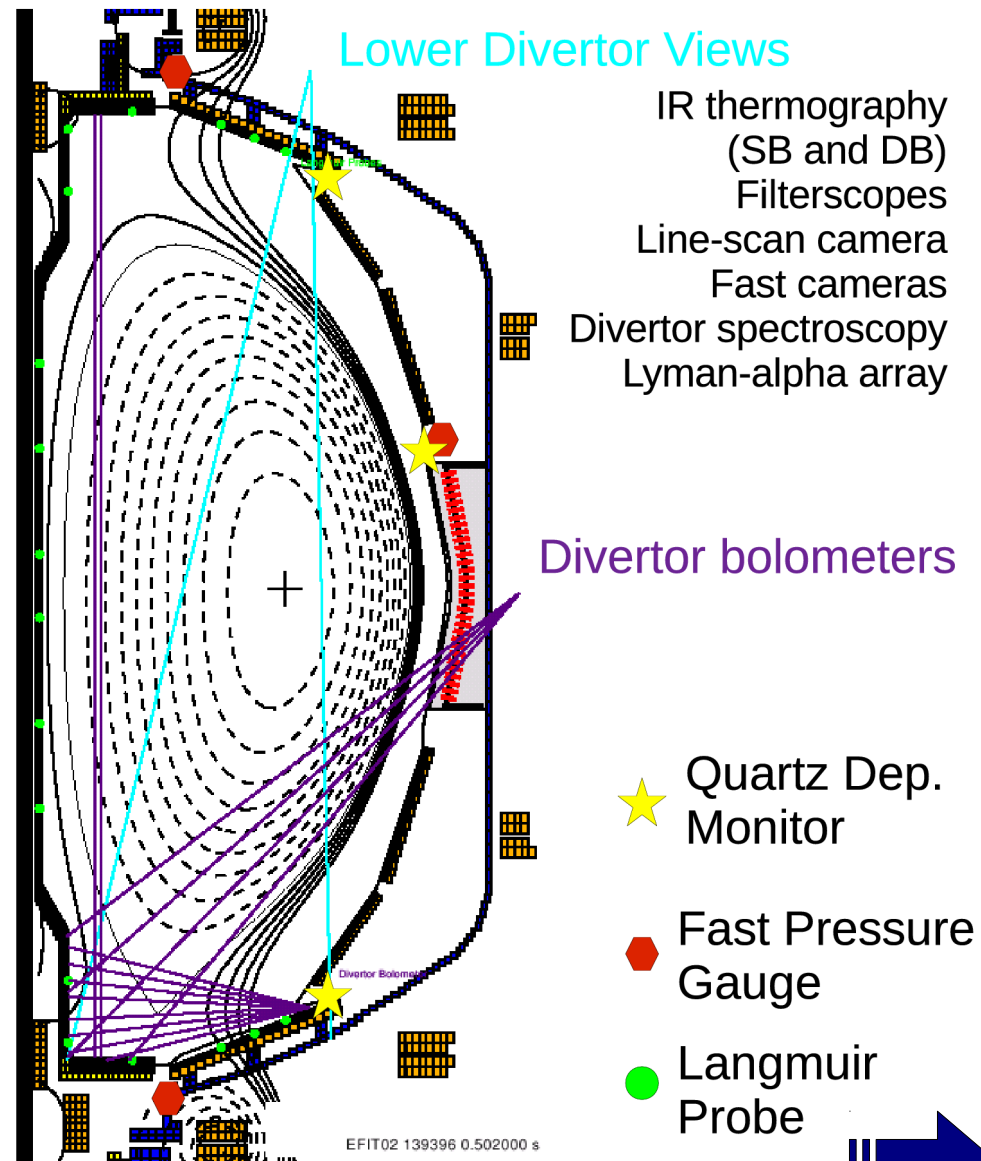


Option SOL-13 – Pseudo Self-Consistent Integration

- Integrates only some of the conservation equations along the flux tube
 - Integrates $T(s)$ along flux tube with a prescribed radiative power loss along flux tube
 - Utilizes ionization model to integrate $\Gamma(s)$ (particle flux) in similar fashion
 - Solves for density and velocity based on pressure balance and flux
- Primary difference with SOL-22 option is that SOL-22 integrates all three conservation equations simultaneously
- For the case run shown, no radiation is prescribed and only the ionization is set as a decaying exponential with decay length of 8cm (compared to 14m distance to mid-plane very close to separatrix)

Wide Range of Diagnostics Available for Constraints

- Each new diagnostic provides means for constraining the model
 - e.g. divertor spectroscopy provides impurity information
 - e.g. QDMs provide impurity redeposition/transport
 - e.g. Pressure gauges provides information on neutrals
- HDLP not shown in figure
 - Inboard coverage by Langmuir probes could still be improved
 - Mid-plane reciprocating probe also not shown



First Sanity Check: LLD Plate Heating

- Thermocouples measure LLD plate temperatures in bulk copper
 - Treat each LLD plate as a 90lb. Calorimeter
 - Rise in mean temperature yields energy deposited over entire discharge
- Estimate plasma heating time by the time spent diverted
- Plate heating and Langmuir probe-based heat flux calculations show particle heating accounts for ~90% of total heat input

$$\Delta E_{plate} = V_{plate} \rho_{Cu} C_{p,Cu} \Delta T$$

$$\Delta E_{plate} = 5222 \text{cm}^3 \cdot 8.94 \frac{\text{g}}{\text{cm}^3} \cdot 0.384 \frac{\text{J}}{\text{g} \cdot \text{K}} \Delta T$$

$$\Delta E_{plate} = 17.9 \text{ kJ/K} \Delta T$$

$$\Delta E_{div} = \Delta E_{plate} \cdot \frac{2\pi}{\theta_{plate}}$$

$$\Delta E_{div} = \Delta E_{plate} \cdot 4.36$$

$$\bar{P}_{div} = \frac{\Delta E_{div}}{\tau_{div}}$$

where τ_{div} = Period of time plasma is diverted

For shot 139396

$$\tau_{div} \approx 0.85[\text{s}] \quad \Delta T_{plate} \approx 8[\text{C}]$$

$$\bar{P}_{div} \approx \frac{4.36 \times 143[\text{kJ}]}{0.85[\text{s}]} \approx 735[\text{kW}]$$

$$P_{OSM-LP} = 674[\text{kW}] \approx 92\% \text{ of } \bar{P}_{div}$$

Study Methodology

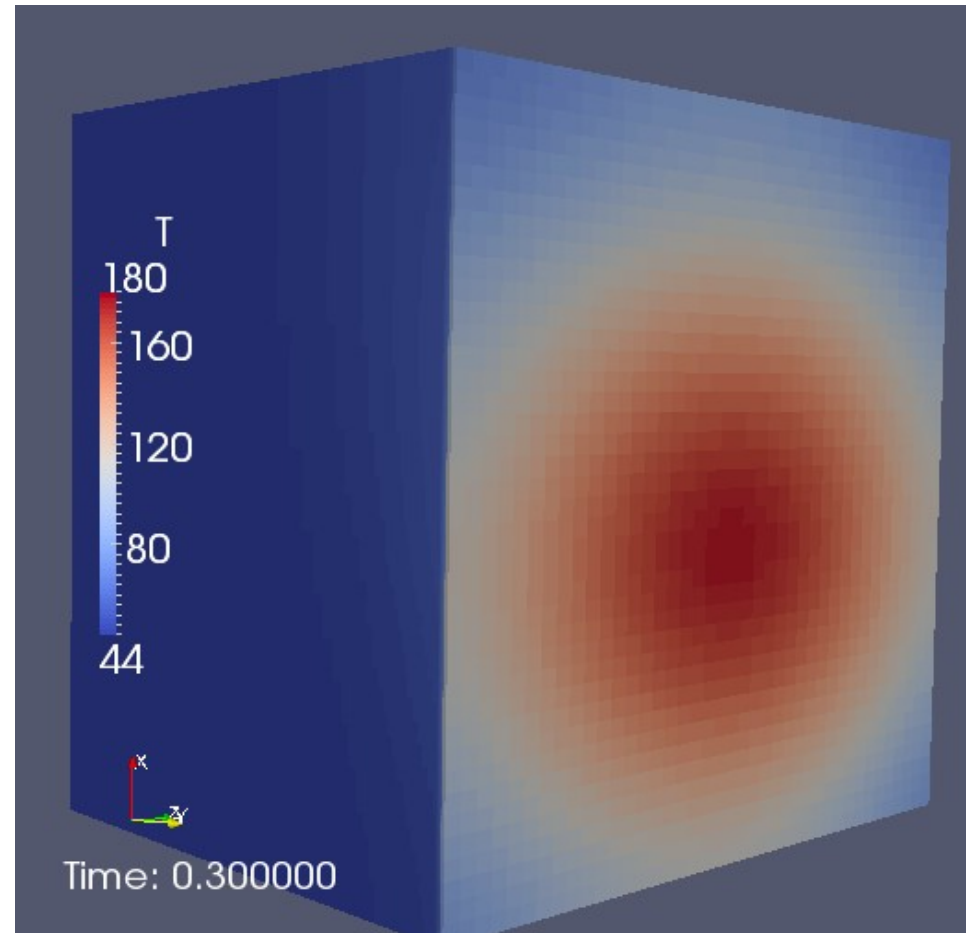
- Take all available data to constrain the plasma and impurity levels
- Determine best material model (e.g. recycling coeff.) to best match available data
- Construct recycling coefficient database for lithiated graphite as well as lithium-coated moly/LLD for range of operating scenarios
 - Local plasma temperature, density
 - PFC bulk and front-face temperature
- Create model to describe the resulting behavior based on the plasma response to the PFCs
 - Supplement with sample diagnosis as it becomes available (see MAPP probe poster BP9.00088)
 - Other offline experiments and modeling as appropriate



Determining LLD Plate Front-Face Temperature Response with Offline Experiments

- Diagnostic neutral beam exposures of LLD sample piece
 - Obtained front-face temperature response to $\sim 1.5\text{MW/m}^2$ heat flux
 - See T. Abrams BP9.00045 for experiment details
- Perfect material bonds not present in sample
 - Tests show much larger temperatures than expected
 - Preliminary estimates indicate resistive layer exists between LLD layers (equivalent to x20 reduction in porous moly conductivity)
- Bench-marked model in the works for future predictive capability

OpenFOAM LLD Sample Model



Extending the Recycling Model

- Simple model may explain steady trend in Li-ATJ data
- Better modeling of the PFCs will depend on extracting actual values of recycling coefficient, not relative recycling
- Some temperature scans already performed
 - Include surface evaporation and recombination
 - Sputtering of lithium and deuterium
 - Sputtering of other impurities
- Informs on PFC choice and conditioning method for NSTX-U and other machines
 - Does liquid lithium saturate in a similar fashion?
 - What are the limits in temperature for “low” recycling to persist?
 - Is there a feasible liquid lithium PFC in a high-performance machine or pilot plant?

Summary

- NSTX divertor is rich in physics topics and phenomena
- Measurements to date indicate LLD interaction with the bulk plasma is subtle and requires careful analysis
 - Some indications of SOL changes via Langmuir probe measurements, however...
 - Complicated by multiple variable changes (e.g. fueling rate)
 - Latest set of data under analysis
- Relative recycling measurement indicates LLD and Li-ATJ PFCs evolve in time over the period of several discharges
 - Corroborates “control room” wisdom that Li wall effects are short lived
 - Analysis of cumulative fluence to PFCs motivates a simple recycling model based on material saturation
 - While encouraging, should be improved with “real” recycling analysis
- OEDGE analysis of NSTX plasmas ramping up after initial test runs – major goal is to develop detailed understanding of lithiated PFCs and the impact on the global plasma

Reprints
